Textures and Microstructures, 2001, Vol. 35, pp. 23–38
Reprints available directly from the publisher
Photocopying permitted by license only

EFFECT OF ZONAL ISOLATION ON THE KINETICS OF SINTERING A PARTICULATE BODY

E.Y. NURKANOV*, R.M. KADUSHNIKOV and V.V. SKOROKHOD

Urals State Technical University-UPI, 19 Mira Street, Ekaterinburg, 620002, Russia

(Received 13 November 2000; In final form 15 January 2001)

This paper describes the so-called meso-scale simulations of sintering a particulate body. Computations were made using 3D structure-imitation computer model of evolution of a powder compact during sintering. It was demonstrated, that in powder bodies the effect of zonal isolation (forming separate groups of particles during sintering) determines features of shrinkage and internal structure of a compact. In case of the diffusion-viscous flow of particles the fact was proved that the zonal isolation is predetermined by ratio of viscosity and free surface energy. It was verified, that there is a critical value of the above ratio with respect to which the balance of internal structure-creating processes is determined.

Keywords: Structure-imitation model; Powder; Particulate body; Sintering; Zonal isolation

INTRODUCTION

Zonal isolation or localization of densification upon sintering of particulate bodies is a well known phenomenon in powder metallurgy which was discovered and generalised as a law of zonal isolation in sintered particulate bodies by Balshin (1972). In real powder systems, zonal isolation plays a key role in the process of shrinkage and in

*Corresponding author.

the kinetics of sintering of a compact as a whole. This effect manifests itself more distinctly, the higher are the rate of densification of local areas with small pores and the powder dispersity.

Existing models of qualitative and quantitative description of the state of a sintered particulate body do not allow precise identification and qualitative assessment of zonal isolation. It refers to the known method of finite elements, and reological macromodelling methods connected with the use of continuum mechanics. (Green, 1972; Skorokhod, 1972; Shima and Oyane, 1976; Tvergaard, 1982; Olevsky, 1998). The above methods employ a macroscopic approach which treats a particulate body as either a continuum or a combination of the phase of substance and the phase of voids. But real particulate bodies are discrete media, even in the case of intensive pressing of powder. Analysis of the real pressed powders (Geguzin, 1984) shows that owing to internal friction and the arch effects, there takes place non-uniform plastic deformation of contacts between particles both inside a compact and on its periphery. Particles of a relatively regular form with a convex surface inside the compact have a substantially less-stressed state, and, correspondingly, lower level of deformation in the by-contact area. Inside the real compact, there is a fair number of contacts where the particles only touch each other or will touch each other in the case of insignificant shrinkage (Skorokhod and Solonin, 1984). In the zone with an increased number of small-area contacts, the Laplace capillar forces become substantially higher than on average over the compact, which results in increased rates of initial shrinkage and, just, isolation of particles into separate groups or clusters. Hence, it is possible to make a conclusion that the zonal isolation should be considered to primarily result from a discrete organization of a particulate body.

Approximation of discrete organization allows one to apply "particles model" (Hockny and Eastwood, 1987) to simulate behaviour of a given group of materials, where the bulk localization takes place most probably. The simulation involves construction of an adequate mathematical model, its implementation in the form of a computer model, and, finally, performance of a series of computations.

Extensive investigations of zonal isolation in the course of sintering were performed on computer models of two-dimensional particles in the works (Kadushnikov and Alievsky, 1989; Kadushnikov *et al.*,

1991a,b). By means of computations, the main regularities of zonal isolation as a topological transition upon microstructure evolution were determined. In the works (Kadushnikov and Alievsky, 1989; Kadushnikov *et al.*, 1991a,b), the concepts of the critical behaviour of a discrete system upon zonal isolation were formulated. In publication (Kadushnikov and Skorokhod, 1991) the authors specified the critical rate of two-particle coalescence in a system of particles. Depending on whether the rate of two-particle coalescence is more or less than the critical one, the system either decomposes into separate groups, or shows up the ability to homogenous sintering.

In the present work, basing on the ideas specified in (Kadushnikov and Alievsky, 1989; Kadushnikov *et al.*, 1991a,b; Kadushnikov and Skorokhod, 1991), the authors made an attempt to study the critical behaviour of particulate bodies upon zonal isolation using a computer model sintering of three-dimensional spheric particles. As main trends of the investigation, searching for critical ratios of the material's phenomenological constants and detection of topological transformations that correspond to the found critical values of constants were chosen.

MODEL DESCRIPTION

Computer-assisted structure-imitating model of sintering spherical particles (Kamenin *et al.*, 1998), which represent the sintering process in three stages, filling, sintering, recrystallization and normal grain growth, is used for computations.

At the filling stage, an initial disordered medium is formed. The initial disordered medium or particulate body is represented as irregular close packing of spherical particles. To construct close packing of different-size spheres in a flat-wall bunker, the following algorithm is suggested. Spheres are generated according to a given law of size distribution and are dropped into the bunker either from one and the same point, or from randomly chosen positions. As soon as the dropped sphere encounters an obstacle, the bunker wall or already packed sphere, it sticks to it (without hitting) and begins to slide on its surface in the direction of the minimum potential energy to the following obstacle. (This direction is a projection of the free-fall direction

on the obstacle surface.) The movement of the sphere stops, either at a point of intersection of 3 surfaces (3 spheres, 2 spheres and 1 plane and etc.) or on the surface perpendicular to the direction of the sphere free-fall (for example, on the bottom of the bunker).

The constructed close packing of spheres is employed in the second stage – simulation of the sintering evolution of spheres. When deriving the equations of motion and dynamics of sizes for the sintered spheres, the aim was to satisfy the equations of sintering kinetics for each pair of contacting spheres in a system. Initial particulate body is represented by a random close packing of N spherical particles: $S_i(R_i, \mathbf{r}_i, \mathbf{v}_i)$, $i = 1, N$; R_i are the radii of spheres, $\mathbf{r}_i$ are the coordinates of their centres, $\mathbf{v}_i$ are the velocities of spheres located in a bunker which is bounded by K flat walls: $(\mathbf{r}, \mathbf{b}_j) = D_j$, $j = 1, K$; $\mathbf{b}_j$ are the normals to the walls.

Upon contacting spheres, their interaction resulted in sintering, should be taken into account. The distance between the centres of the contacting spheres is:

$$|\mathbf{r}_{ij}| = |\mathbf{r}_i - \mathbf{r}_j| < R_i + R_j. \tag{1}$$

The equation of sintering kinetics for all pairs of incidental (contacting) spheres can be written in the following form:

$$\mathbf{v}_{ij} = \dot{\mathbf{r}}_{ij} = f\left(|\mathbf{r}_{ij}|\right)\mathbf{r}_{ij}, \quad i = 1, N; \; j \to i \tag{2}$$

(the last entry means that "j is incidental (contacting) to i"). To use condition 2 as a "tendency" for the motion of a system of spherical particles, the equations of motion (Kamenin *et al.*, 1998) should look as follows:

$$\begin{cases} \dot{\mathbf{r}}_i = \mathbf{v}_i - \mu \sum\limits_{j \to i} \left(\mathbf{v}_{ij} - f\left(|\mathbf{r}_{ij}|\right)\mathbf{r}_{ij}\right)\left(f\left(|\mathbf{r}_{ij}|\right) + f'\left(|\mathbf{r}_{ij}|\right)|\mathbf{r}_{ij}|\right) \\ \dot{\mathbf{v}}_i = \dfrac{\mathbf{F}_i}{m_i} - 3\dfrac{\mathbf{v}_i|\dot{\mathbf{r}}_i|}{R_i|S_i|} \cdot \Xi_i - \mu \sum\limits_{j \to i} \left(\mathbf{v}_{ij} - f\left(|\mathbf{r}_{ij}|\right)\mathbf{r}_{ij}\right) \\ \dot{R}_i = \dfrac{|\dot{\mathbf{r}}_i| \cdot \Xi_i}{|S_i|}. \end{cases} \tag{3}$$

where $m_i = 4/3\pi\rho R_i^3$, ρ is the density of the spheres' material, $\mathbf{F}_i$ is the sum of the external forces affecting each sphere; μ is the weight multiplier actually responsible for the sintering effect on the motion of the

system of spheres, $|S_i| = \int_{\Phi_i} \int ds = \partial V/\partial R_i$ is the area of the free surface ϕ_i of the ith sphere, $\partial V/\partial r_i = \Xi_i = \int_{\Psi_i} \int \dot{\mathbf{r}}_i/|\dot{\mathbf{r}}_i|\,\mathbf{n}\,ds$ can be interpreted as the projection area of the occupied surface ψ_i of the ith sphere on the plane normal to $\dot{\mathbf{r}}_i$ ($\mathbf{n}$ is the unit vector of the normal to the surface), V is the volume of spheres' packing. The third stage is entirely controlled by the motion and sintering of the spheres, that is why it is necessary to continue integrating the system of Eqs. (3). The effects of the normal grain growth are reflected only in the equations for dynamics of sphere sizes; namely, for the spheres with the surface fully covered by the neighbours (not affecting the mass conservation), the equations of dynamics of normal grain growth are used:

$$R_i = \lambda \sum_{j \to i} \left(\frac{1}{R_i} + \frac{1}{R_j} \right). \tag{4}$$

Thus, at a certain instance t, the state of a physical system is described by a set of positions and velocities of the particles $\{\mathbf{r}_i(t), \mathbf{v}_i(t), i=1, N\}$. The time step cycle recalculates these values using the interaction forces and equations of motion to obtain the state of the system at a later instance $t+dt$.

The function $f(|\mathbf{r}_{ij}|)$ should specially be dwelt on; it is determined as follows:

$$\mathbf{v}_{ij} = f\left(|r_{ij}|\right)\mathbf{r}_{ij}, \quad f\left(|r_{ij}|\right) = \frac{B}{m\varepsilon(1-\varepsilon)^{m-1}}, \quad \varepsilon = \frac{|\mathbf{r}_{ij}|}{|\mathbf{r}_{ij}^{(0)}|}. \tag{5}$$

The expression (3) can be derived by differentiating with respect to time the known phenomenological formula (Geguzin, 1984) describing the kinetics of the initial stage of mutual sintering of spherical particles

$$\left(\frac{|\mathbf{r}_{ij}|}{|\mathbf{r}_{ij}^{(0)}|} \right)^m = Bt, \tag{6}$$

where $\mathbf{r}_{ij}, \mathbf{r}_{ij}^{(0)}$ are the current and the initial distances between the centres of contacting particles, B and m are the constants determined by the type of substance and the mass transfer mechanism. For the

mechanism of viscous flow

$$m = 1, \quad B = \frac{\lambda}{|\mathbf{r}_{ij}^{(0)}|}, \quad \lambda = \frac{3\sigma}{4\eta} \tag{7}$$

where η is the viscosity coefficient, σ is the surface tension (specific surface energy), λ is the actual initial rate of approaching the centres of contacting spheres.

ANALYTIC DETERMINATION OF THE EFFECTIVE TIME OF SINTERING

The values η and λ may vary for different real materials by several orders, depending on the sintering temperature, crystallinity of the material and, etc., which leads in computer experiments to a significant scatter of times of integrating the system of Eq. (3). It is necessary to determine such dimensionless effective time of sintering (integrating) which would correspond to equivalent states of the dynamic systems consisting of spherical particles with different viscous and energetic properties. Let us determine the effective time of sintering as a time required for the Laplace forces in systems with the same initial configuration of particles and different viscous and energetic properties to perform the same amount of work on shifting particles to the sought energetically favourable configuration, may vary for different real materials by several orders, depending on the sintering temperature, crystallinity of the material and, etc., which leads in computer experiments to a significant scatter of times of integrating the system of Eq. (3). It is necessary to determine such dimensionless effective time of sintering (integrating) which would correspond to equivalent states of the dynamic systems consisting of spherical particles with different viscous and energetic properties. Let us determine the effective time of sintering as a time required for the Laplace forces in systems with the same initial configuration of particles and different viscous and energetic properties to perform the same amount of work on shifting particles to the sought energetically favourable configuration.

Let us consider two systems with similar initial configuration and characteristics $[\sigma, \lambda]$ and $[\sigma', \lambda']$, with $\lambda' = \omega\lambda$. The work to move the

ith particle in a time $\Delta\tau$ equals to

$$\Delta W_i = \mathbf{v}_i \mathbf{F}_L \Delta\tau, \tag{8}$$

where $\mathbf{v}_i$ is the velocity of the ith particle centre, $\mathbf{F}_L$ is the pressing force in the zone of two-particles contact. According to (Balshin, 1972), the following formula for $\mathbf{F}_L$

$$\mathbf{F}_L = 2\pi\sigma R \tag{9}$$

is valid for $X \leq 0.5R$ (X is the radius of the contact zone, R is the radius of a particle), and the condition for the work equality in both systems considered is expressed as follows:

$$\begin{aligned} \Delta W_i &= \Delta W'_i \\ \sigma \mathbf{v}_i \Delta\tau &= \sigma' \mathbf{v}'_i \Delta\tau'. \end{aligned} \tag{10}$$

Going over to the differential Eq. (3), and omitting the second-order terms $O(\Delta t^2)$ we have:

$$\begin{aligned} \mathbf{v}_i^{(n)} &= -\mu \sum_{j \to i} \left(\mathbf{v}_{ij}^{(n-1)} - \lambda \frac{\mathbf{r}_{ij}^{(n-1)}}{|\mathbf{r}_{ij}^{(n-1)}|} \right) \Delta t - \mathbf{v}_i^{(n-1)} \\ \mathbf{v}_i^{(1)} &= -\mu\lambda \frac{\mathbf{r}_{ij}^{(0)}}{|\mathbf{r}_{ij}^{(0)}|} \Delta t \end{aligned} \tag{11}$$

where $\mathbf{v}_i^{(1)}$ is the initial velocity of the ith particle, $\mathbf{v}_i^{(n)}$ is the velocity of the particle on the nth step of iteration. Taking into account that

$$\begin{aligned} \lambda' &= \omega\lambda \\ \mathbf{v}_i^{(1)\prime} &= -\mu\omega\lambda \frac{\mathbf{r}_{ij}^{(0)}}{|\mathbf{r}_{ij}^{(0)}|} \Delta t = \omega \mathbf{v}_i^{(1)} \end{aligned} \tag{12}$$

one can write

$$\mathbf{v}_i^{(n)\prime} = \omega \left[-\mu \sum_{j \to i} \left(\Phi(\mathbf{v}_{ij}^{(1)}) - \lambda \frac{\mathbf{r}_{ij}^{(n-1)}}{|\mathbf{r}_{ij}^{(n-1)}|} \right) \Delta t - \psi(\mathbf{v}_i^{(1)}) \right] = \omega \mathbf{v}_i^{(n)} \tag{13}$$

Substituting (13) into (10), we have

$$\begin{aligned} \sigma N \Delta t &= \sigma' \omega N' \Delta t' \\ \sigma \lambda \Delta \tau &= \sigma' \lambda' \Delta \tau', \end{aligned} \tag{14}$$

where Δt is the iteration step, N is the number of iterations.

Let us introduce a series of additional designations. If the condition (14) is fulfilled, the value Ω is determined as the effective time of sintering for systems with characteristics $[\sigma, \lambda]$ and $[\sigma', \lambda']$, and value β is the conditional rate of sintering. If W is the full work of internal forces, then Ω is the dimensionless effective time of sintering or a number of sintering periods. For Ω sintering periods in systems $[\sigma, \lambda]$ and $[\sigma', \lambda']$, internal forces perform the same work on moving particles.

$$\begin{aligned} W &= \Omega \sigma \lambda \Delta \tau \\ \beta &= \sigma \lambda. \end{aligned} \tag{15}$$

ANALYSIS OF THE COMPUTATION RESULTS

Let us assess degree of the effect that β exerts on zonal isolation, dynamics of densification and shrinkage parameters. In this paper we confine ourselves to the investigation of the case of $\sigma \approx \sigma'$. Let us determine the upper limit of the effective sintering time as $\Omega < \Omega_b$, where Ω_b is the value corresponding to the recrystallization onset. Recrystallization, as applied to computations, is the process of joining particles and decreasing their overall number.

For β from the range $[10^{-3}; 10^{5}]$ and $\Omega < \Omega_b$, series of computations on sintering of a close packing (further on referred to as "package") were performed. The package consisted of 1000 particles of the same diameter ($N = 1000$, ASD $= 0.0$, $R = 1.0$, cubic bunker with 16×16 base). The compacted bulk was assessed using the following parameters: Ls is the relative linear shrinkage of the package, Vs is the relative volume shrinkage of the package, α is the parameter of shrinkage:

$$\alpha = \frac{\gamma - \gamma_0}{1 - \gamma_0} \tag{16}$$

where γ is the relative density, and γ_0 is the initial relative density. The relative density was determined as $\gamma = V_{0.5}/0.5V$, where V is a volume of a compact, $V_{0.5}$ is the volume of particles in a parallelepiped with a volume of $0.5V$, which is cut from the central part of the package.

In the course of computations over the whole range of β variation, the effect of localization of densification clearly manifested itself (see Fig. 1a and b). Two simultaneous competing processes were observed: the process of joining particles into separate groups and motion of separate groups toward the mass centre of the package, and the balance of the processes was determined just by β value rather than by the uniform distribution of the particles contacts, because one and the same initial packing was used for all computations. Specific features of the zonal segregation connected with β were noted.

Analysis of the computation results (see Fig. 2) showed that there is a critical value of β_{cr} which in the case of modelling under consideration

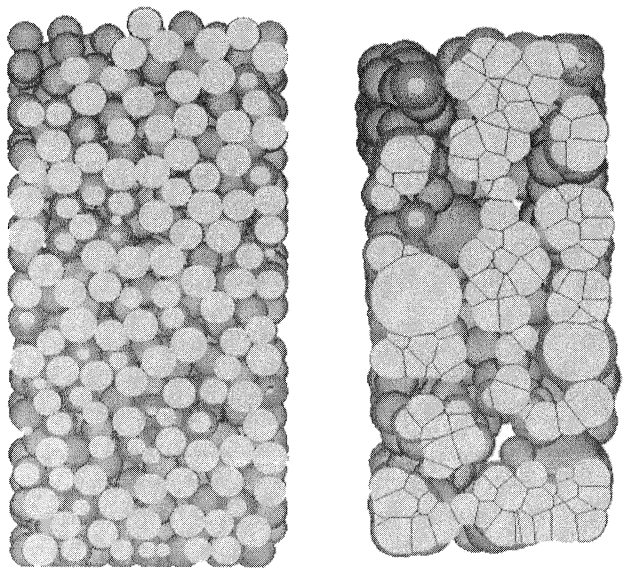

FIGURE 1 Section of a package of spherical particles ($N = 1000$, ASD $= 0.0$, $R = 1.0$, cubic bunker with 16×16 base). Cross-cut of the particles is in grey. (a) Before sintering; (b) after sintering.

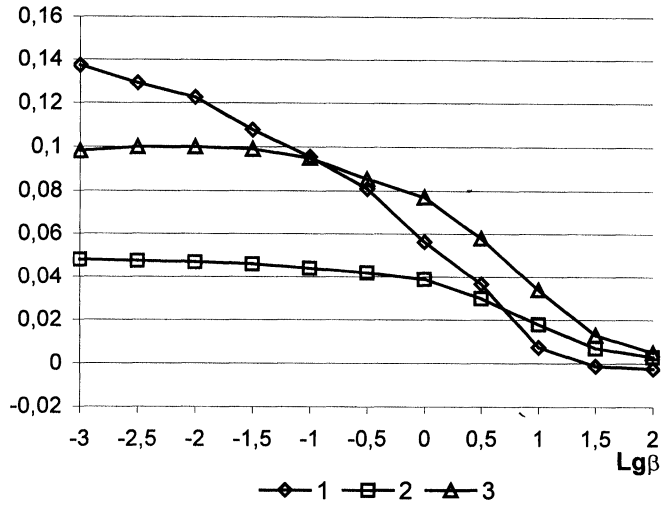

FIGURE 2 Dependencies of parameter of shrinkage α, relative linear shrinkage Ls, and relative volume shrinkage Vs from β. Effective time $\Omega = 1$. (1) α; (2) Ls; (3) Vs.

made up $\beta_{cr} \approx 25 \div 30$. At values lower than β_{cr}, the process of external shrinkage in the whole range of sintering was accompanied by internal densification. At higher values, the slowing-down of external shrinkage and decompaction (increase of porosity) were observed. Positive internal densification manifested itself only at the final stage of sintering. It is worth noting that the negative densification ($\alpha < 0$) or the package growth is an effect that was registered in a number of natural experiments (Balshin, 1948). Thus, the β_{cr} value divides model particulate systems into two categories: a) systems with external shrinkage and internal densification, and b) systems with external shrinkage and internal decompaction.

Based on the conditions of calculating α a conclusion can be made concerning the features of topological transformations of the internal structure depending on β. At $\beta > \beta_{cr}$, the parameters of shrinkage and densification have opposite signs. Linear shrinkage and volume shrinkage (Ls > 0, Vs > 0) are calculated over the whole volume and, therefore describe the total shrinkage of the package, whereas the densification parameter ($\beta > \beta_{cr}$, $\alpha < 0$) is determined in the central part of the package with its volume equal to $0.5V$ (where V is the total

volume). Thus, a decrease in the density inside the central volume $0.5V$ indicates that particles leave this zone and move toward the centres of corresponding separate groups. Since the external shrinkage in this case is insignificant (fractions of percent), it is possible to conclude that the rate of shrinkage inside the group is higher than the rate of moving separate groups towards the mass centre of the package.

When $\beta \leq 1$ (see Fig. 3), in the analysed range of β, the average radius of contact area X and the average distance between the particles D during the time $\Omega = 1$ reach almost the same values, $0.55R$ and $1.64R$, respectively. When $\beta > 1$, the average values of X and D did not exceed $0.03R$ and $1.99R$, respectively, for the time $\Omega = 1$. This fact testifies to the following. In publication (Kadushnikov and Skorokhod, 1991), an assumption was made on the existence of a zone of coherent sintering, the minimum size of which is a constant for a given type of substance, geometrical structure and the mechanism of two-particle coalescence.

However, it is rightful to make an assumption that besides the minimal possible size of a separate group in a sintered particulate system, the maximal possible size exists. In accordance with this assumption, the linear portion of the dependencies $D(\mathrm{Lg}\,\beta)$ and $X(\mathrm{Lg}\,\beta)$ (see Fig. 3) indicates that the sintered system reached the state with the maximal characteristic size of a cluster. Correspondingly, the decrease of D and X (see Fig. 3) seems to be a result of the cluster fragmentation

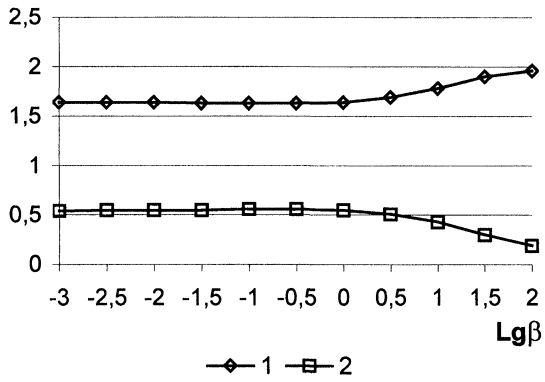

FIGURE 3 Dependencies of average distance between the centres of contacting particles D and average radius of contact area X from β. (1) D; (2) X.

and refinement. Indeed, the experiments results showed (see Fig. 4) that under condition $\beta > \beta_{cr}$ (for $\Omega = 1$), there is an effect of decreasing the average size of clusters together with increasing their total number and for, the increase and stabilisation of an average cluster size were observed (see Fig. 4).

With the further increase in the conditional rate of sintering up to the level of $\beta \gg \beta_{cr}$, substantial changes were noted in the character of zonal isolation, densification, and shrinkage compared with the pre-critical and critical ranges of β. On growing β (Figs. 5 and 6) the rate of topological transformations in the package decreased (the parameter per unit effective time of sintering Ω changes). At the earlier stages of sintering, along with an insignificant external volume and linear shrinkage, the internal decompaction took place. The degree of decompaction was weakly sensitive to the decrease of β by an order (from 10^4 to 10^5) that was proven by the minima in the graphs $\alpha(\Omega)$ (Fig. 5). Besides, close values of the external shrinkage ($Vs \approx 2.5\%$) corresponded to the minima of $\alpha(\Omega)$. In the authors' opinion, this result is probable only when the system reaches the structural state with a minimal size of a cluster. Indeed, if we consider the parameter α to have manifested itself as a measure of the densification increase and the porosity growth, then the end of the α fall (minimum in the $\alpha(\Omega)$ graphs) means that the pores among the groups were eventually formed and reached the limiting size. As was established earlier, the growth of pores among the groups was related to the process of the joining particles into small separate groups. It is evident that the greater number of clusters that occurred in a unit volume, the larger was the area of a free surface and, hence, more the porosity. Consequently, if the porosity has the maximal value, the number of clusters is maximal, and the cluster size is minimal.

Since the increase of β causes the cluster refinement to a certain minimal size, it was logical to suppose that the minimum cluster size is controlled solely by the irregularity degree of the initial structure and is limited from below by the value $4\pi R^3 K/3$, where K is the average coordination number of the close packing. Moreover, as upon decreasing the size of separate groups their number in a given volume substantially increased, it was logical to suppose that the rigid carcass of clusters was formed inside the sintered compact, hindering movement of a single cluster toward the mass centre of

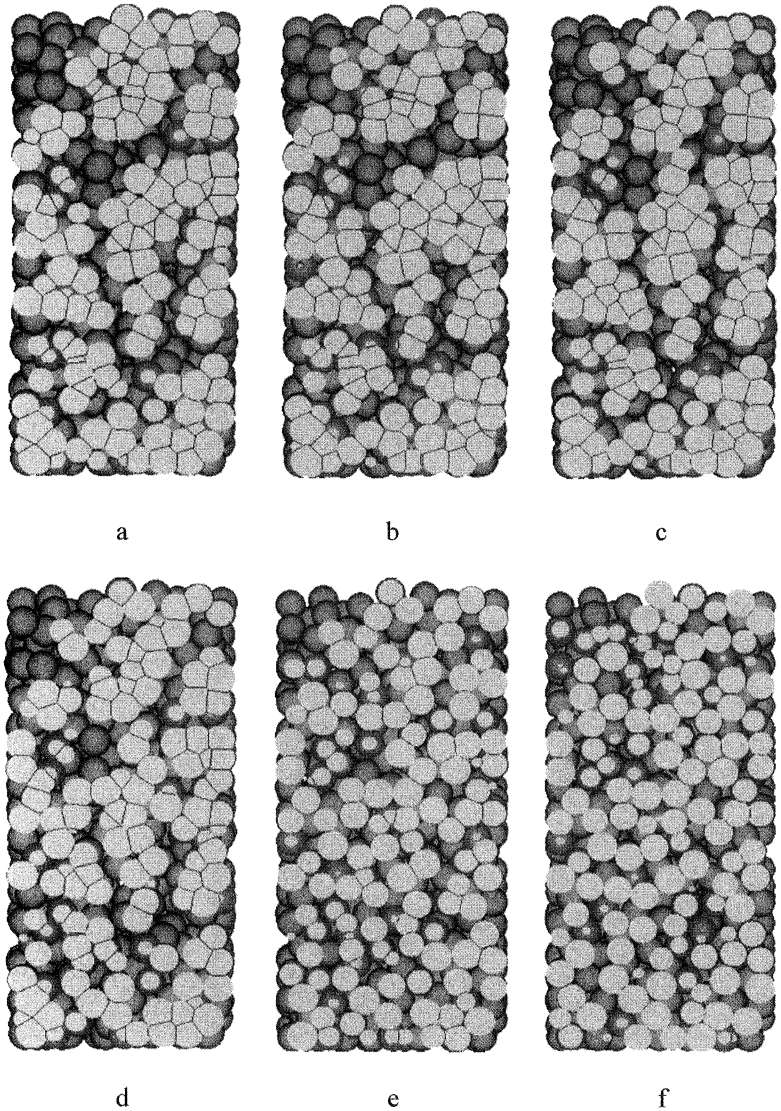

FIGURE 4 Section of a sintered package of spherical particles. Effective time $\Omega = 1$. (a) $\mathrm{Lg}\beta = 10^{-3}$; (b) $\beta = 10^{-2}$; (c) $\beta = 10^{-1}$; (d) $\beta = 1$; (e) $\beta = 35$; (f) $\beta = 10^{2}$.

the compact. The shrinkage of the compact proceeds primarily at the expense of the shrinkage inside the groups, and this gives an explanation to the low level of densification at $\beta \gg \beta_{cr}$.

Another feature of the sintering at $\beta \gg \beta_{cr}$ should be pointed to. The duration of the topological transformations accompanied by the densification and shrinkage grows in the units of Ω with increasing β. For example, for $\beta = 1$ the boundary value of $\Omega_b \approx 2$, and for $\beta = 10^5$ $\Omega_b \approx 120$. For $\beta = 10^5$ the value of Ω_b corresponds to a jumplike growth of the shrinkage Vs (see Fig. 5). Proceeding from the definition of Ω, one can conclude that the work of internal forces moving particles towards the energetically effective configuration grows with increasing β despite the fact, that the viscosity of the particles' material decreases, i.e. the ability of particles of coalescence increases. As it was noted above, at increased values of $\beta \gg \beta_{cr}$, the most probable is the appearance of the rigid carcass consisting of the minimum-size clusters. The above carcass prevents the cluster motion, as a whole, and this leads to an increased work of the internal forces.

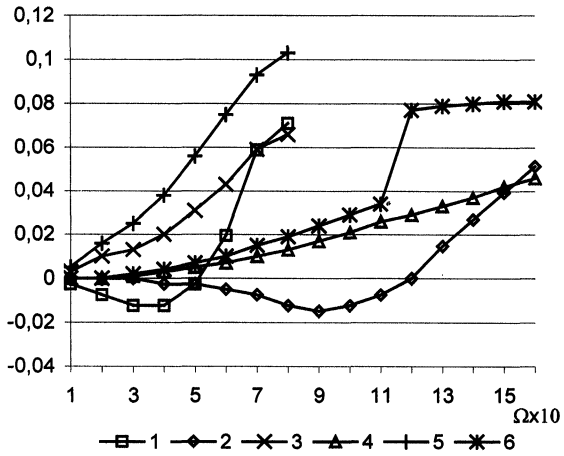

FIGURE 5 Dependencies of parameter of shrinkage α (1, 2), relative linear shrinkage Ls (3, 4) and relative volume shrinkage Vs (5, 6) from effective time of sintering Ω at $\beta \gg \beta_{cr}$. (1) $\beta = 10^4$; (2) $\beta = 10^5$; (3) $\beta = 10^4$; (4) $\beta = 10^5$; (5) $\beta = 10^4$; (6) $\beta = 10^5$.

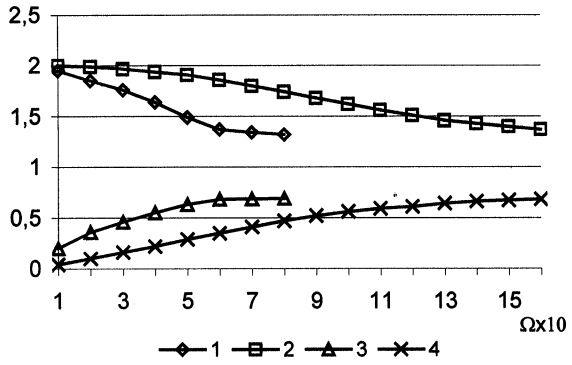

FIGURE 6 Dependencies of average distance between the centres of contacting particles D (1,2) and average radius of contact area X (3,4) from effective time of sintering Ω at $\beta \gg \beta_{cr}$. (1) $\beta = 10^4$; (2) $\beta = 10^5$; (3) $\beta = 10^4$; (4) $\beta = 10^5$.

CONCLUSION

Thus, for the sintered particle systems with the diffusion-viscous mechanism of the two-particle coalescence, the following regularities can be considered to be the most common and established:

a) The effect of zonal isolation is clearly pronounced in the range of $[10^{-3}; 10^5]$;
b) There exists a β_{cr} value with respect to which the balance of internal structure-creating process is determined; at $\beta > \beta_{cr}$ the balance shifts towards the formation of small separate groups and shrinkage inside the groups upon retardation of the total external shrinkage; at $\beta > \beta_{cr}$ the balance shifts towards the process of consolidation of separate groups and their preferable motion towards the mass centre of the package, which increases the homogeneity of sintering;
c) The initial degree of the close packing irregularities and the β value control the characteristic size of a cluster and this size is limited not only from below, but also from above;
d) At $\beta > \beta_{cr}$ the total work of internal forces on moving particles towards the energetically effective configuration increases; at $\beta \gg \beta_{cr}$ the rigid carcass of clusters with the minimum size is formed, slowing-down the densification and shrinkage.

References

Balshin, M.Y. (1948). *Powder metals science.* Moscow: Metallurgizdat.

Balshin, M.Y. (1972). *Scientific basis of powder metallurgy and metallurgy of a fiber.* Moscow: Metallurgiya.

Geguzin, Ya.E. (1984). Physics of sintering. Moscow: Nauka.

Green, R.G. (1972). A plasticity theory for porous solids. *International Journal of Mechanical Science*, **4**, 109–120.

Hockny, R., Eastwood, G. (1987). *Computational modelling by particle method.* Moscow: Mir.

Kadushnikov, R.M., Alievsky, D.M. (1989). Computer modelling of liquid-phase sintering processes. In *Computing machinery in physico-technical research.* Sverdlovsk. UPI, pp. 25–28.

Kadushnikov, R.M., Alievsky, D.M. Alievsky, V.M. (1991a). Computer modelling of polydisperse materials microstructure evolution during sintering. I. Basic terms. *Poroshkovaya Metallurgiya*, **2**, 18–24.

Kadushnikov, R.M., Alievsky, D.M. Alievsky, V.M. (1991b). Computer modelling of polydisperse materials microstructure evolution during sintering. II. Zonal segregation. *Poroshkavaya Metallurgiya*, **5**, 5–10.

Kadushnikov, R.M., Skorokhod, V.V. (1991). Research of zonal segregation during the sintering of powder bodies using methods of computer modelling. *Poroshkovaya Metallugiya*, **7**, 31–37.

Kamenin, I.G., Kadushnikov, R.M., Alievsky, V.M., Alievsky, D.M., Somina S.V. (1998). 3-dimensional structure-imitation model of evolution of microstructure of powder body nduring sintering. *Textures and Microstructures*, **32** 221–233.

Olevsky, E.A. (1998). Theory of sintering: from discrete to continuum. *Materials Science and Engineering*, **23**, 41–100.

Shima, S., Oyane, M. (1976). A plasticity theory for porous metals. *International Journal of Mechanical Science*, **6**, 285–291.

Skorokhod, V.V. (1972). *Reological basis of sintering theory.* Kiev: Naukova Dumka.

Shorokhod, V.V., Solonin, S.M. (1984). *Physico-metallurgical basis of powders sintering.* Moscow: Metallurgiya.

Tvergaard, V. (1982). On localization in ductile materials containing spherical voids. *International Journal of Fracture*, **18**, 237–252.